Design and Fabrication of a Low Power Electro-thermal   -sha e Actuator With Large Dis lacement

Jay J. Khazaai, M. Haris M. Khir, Hongwei Qu, James Slicker*

Department of Electrical and Computer Engineering, Oakland University
Rochester, Michigan 48309, USA, jkhazaai@oakland.edu
* MicroStar Technologies, LLC, Bloomfield, Michigan 48324

ABSTRACT

This paper reports the design and microfabrication of a new V-shape MEMS electro-thermal actuators. An electro-thermal model for quick device performance prediction has been developed. The results from the model have good agreement with the numerical simulation results. At 1 volt of driving voltage with a low power consumption of ~2.2 mW, these actuators are capable of delivering large in-plane displacement of ~2.7 µm and large magnitude force of ~240 µN. The proposed V-shape actuator significantly reduces the maximum undesired out-of-plane displacement to less than ~0.006 µm attributed to the structural symmetry. These V-shape actuators fabricated using PolyMUMPS process are suitable for a variety of applications such as RF switches where large forces and long traveling distances are needed.

Keywords: Micro-Electro-Mechanical Systems (MEMS), Electro-thermal Actuators, Modeling, PolyMUMPS, CoventorWare, Finite Element Analysis (FEA)

1 INTRODUCTION

A few actuating principles, including electrostatic, electromagnetic and electrothermal, have been employed in MEMS actuators design. In MEMS switches, electrostatic and electromagnetic devices normally have advantages of fast switching speeds. Electrostatic actuating switches however require significantly large voltage levels but deliver small displacement and contact force. Electromagnetic switches require large actuation power and particular fabrication processes due to the material compatibility with common MEMS materials. Thus, electro-thermal MEMS actuators have found many applications because of their capability of producing large forces, and long traveling distances [1-4]. By selecting a proper material, a lower actuating voltage is possible.

Some MEMS switches, when closing, require large contact forces and reliable connection. The authors have developed a proprietary MEMS switch where a unique latching mechanism is employed for reliable contact. The switch consists of two sets of actuators used as drivers for the contact mechanism and the contact latching system, respectively. With a proper actuating sequence, the programmable switch can be actuated and latched to "ON" and "OFF" states after the actuator power is removed at the end of sequence. To meet the contact and latching requirements, two sets of electro-thermal MEMS actuators with opposite directional displacements have been designed and fabricated. PolyMUMPS process technology was used for device fabrication [5]. The scope of this paper is to report the design and fabrication of the aforementioned thermal devices named as V-shape actuators. Critical design requirements such as large contact force, reliable alignment of the contacts, and less out-of-plane displacement are expected. Due to the technology limitation of 2 µm polysilicon thickness, the design strategy is focused on the realization of large in-plane displacement and small out-of-plane displacement. An analytical model has been created to predict the desired steady-state actuating performance. The analytical results from the developed model are verified numerically by CoventorWare, a comprehensive FEA tool dedicated to MEMS design. The following sections present in detail the structural design, modeling, fabrication process, and test results of the V-shape actuators.

2 DESIGN CONCEPT

Figure 1 illustrates the structural configurations of two new V-shape actuators designed to generate (a) backward and (b) forward displacements. The unique structure of this actuator is basically the combination of a chevron beam actuator and a cold-hot beam actuator with unequal hot beams.

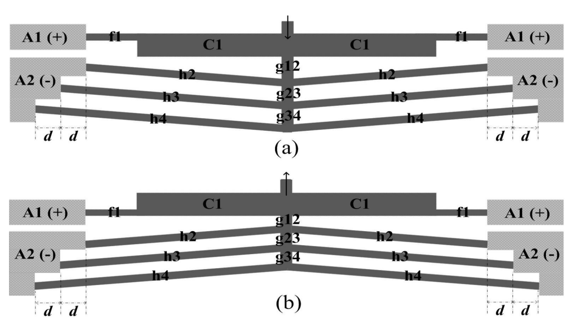

Figure 1: Two types of V-shape thermal actuators, for (a) backward and (b) forward in-plane displacements.

In the proposed V-shape actuators, two modified U-shape actuators shown in Figure 2 are uniquely integrated to create a symmetric structure. The cold arm labeled as *C* has two functions in this structure; to minimize the out-of-plane displacement of the chevron hot beams and to reinitialize the chevron beam displacement as a spring when de-actuated. The uniqueness of this actuator compared to a straight connection [1], is the inclusion of the hot arm, denoted by "*h2*", connected with a central joint beam at an angle of 90°±θ, as shown in Figure 2. The non-perpendicularity between the hot arms and the central beam not only guarantees a desired in-plane directional displacement but also increases traveling distance.

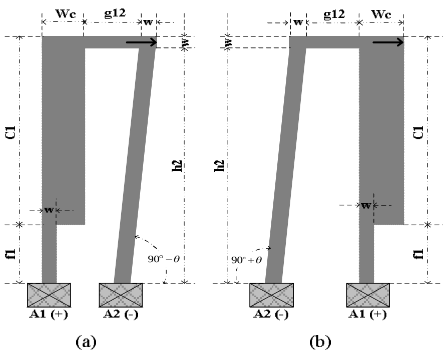

Figure 2: (a) and (b) are two modified U-shape thermal actuators designed for better guiding and larger in-plane displacement.

The angle θ and the length difference *d* of the hot arms play major roles in the optimization of the device performance, a θ = 5° is selected in this design. The major specifications of the V-shape actuator designed for the micro-switch application are tabulated in Table 1. Parameters *f1, C1, h2, h3, h , g12, g23, g3* are referring to the flexure, cold, hot, and joint beams, respectively.

Beams	Si e m	Resis-tance (Ω	Current mA	Power mW
f1	90×2×2	450	1.11	0.567
C1	100×20×2	50	1.11	0.063
h2	190×2×2	950	0.439	0.183
h3	220×2×2	1100	0.366	0.148
h	250×2×2	1250	0.317	0.126
g12	10×2×2	10	2.22	0.050
g23	10×2×2	10	1.40	0.019
g3	10×2×2	10	0.634	0.004
a , b	530×60×2	445	2.22	2.160

Table 1: Structural dimensions and electrical parameters of the thermal actuators in Figure 2. An operating voltage of 1 V is applied.

When electrical current passes through the actuator structure, heat is generated due to resistivity of the polysilicon arms. The electrical power is converted to heat causing the mechanical expansion in actuator structural beams. In our actuator structure, the cross section expansion is very small and has no effect on the application of the actuator. Therefore, the discussion is focused on one-dimensional calculation in which only the length change is considered. The in-plane operating displacement (Y direction) resulted from arm length expansion is analyzed. In the actuator design, the dimensions of the flexure arm are chosen as a reference design parameter. The electro-thermo-mechanical characteristics of the V-shape actuator are determined based on the flexure characteristics.

2 1 Electrical model and analysis

The total resistance of the V-shape actuator, R_t, is a function of the dimensions (length L, width W, and thickness H) of the beams and also the operating temperature. As the temperature of the beams changes, the total resistance of the actuator is also altered. At a fixed voltage, total electrical current and power generated in the actuator is a direct function of the total resistance. Figure 3 illustrates a general lumped-element model and also the relevant electrical model for the V-shape actuators shown in Figure 1. Note that only steady-state response is discussed in this paper.

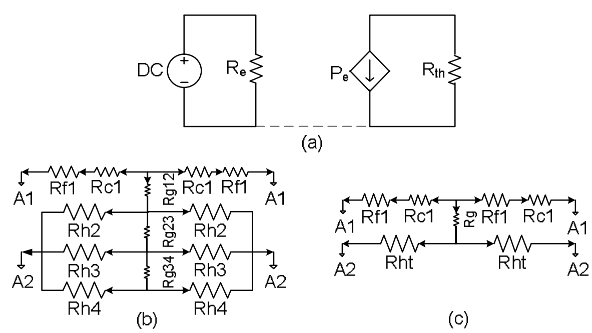

Figure 3: (a) is a general lumped-element model of the V-shape actuators shown in Figure 2, (b) electrical/thermal model, and (c) simplified model.

The electrical resistance of an actuator beam is a function of the material resistivity ρ, and is determined by: R R_0L , where $R_0=\rho$ 10 is the sheet resistance for the polysilicon 1 obtained from the PolyMUMPS technology. Considering flexure *f1* as a reference mechanical design parameter, the size ratio β $(L$ $)$ $(Lf_1$ $f_1)$ can be defined for actuator beams. Applying dimensions defined in Table 1, the size ratios for *f1, C1, h2, h3, h , g12, g23, g3* beams are determined as β_{f1} 1, β_{C1} 0.111, β_{h2} 2.111, β_{h3} $2.$, β_h 2.777, β_g $\beta_{g12}\approx$ β_{g23} β_{g3} 0.022, respectively. The length difference between two adjacent hot-arms *d* and the size ratio is determined by β_d β_h - β_{h3} β_{h3} - β_{h2} 0.333. The size ratios β_{h2}, β_d along with the number of chevron hot-arms, n 3, are set as design parameters. Having the size ratio β_d and β_{h2}, the size ratio for the rest of chevron hot arms can be obtained by $\beta_{h\ i\ 1}$ β_{h2} $(i\text{-}1)$ β_d, for i = 1 to n. In the special design case with three chevron hot arms, the size ratio are given by β_{h3} β_{h2} β_d, and β_h β_{h2} $2\beta_d$. With the known size ratios and the number of arms, i.e., β_{C1}, β_{h2}, β_d, and n, the total resistance of these actuators can be calculated by $R_t = [\beta_{ht} + \beta_g + 0.5(1+\beta_{C1})].R_{f1}$. Due to the fact of small length of gaps between hot-arms compare to length of hot arms (β_g β_d<β_{h2}<β_{h2}<β_h) with a good approximation, the total size ratio β_{ht} of all three chevron hot arms $h2,\ h3,\ h$ can be obtained by the following equation:

$$\beta_{ht} = \frac{\sum_{m=1}^{n=3} \left(0.5\beta_{h2}\right)^m . \left(0.5(m+1)\beta_d\right)^{3-m}}{\sum_{m=1}^{n=3} m.\left(0.5\beta_{h2}\right)^{m-1} . \left(0.5(m+1)\beta_d\right)^{3-m}} \tag{1}$$

2 2 Thermal model and analysis

There are three modes of heat transfer to consider: conduction, convection, and radiation. In this paper, the contributions of heat convection and radiation are relatively small compare to heat transferred by conduction and are ignored. Conduction refers to heat transfer by diffusion through actuator beams, and is analogous to electrical conduction. Thermal energy transfer rate as a function of the temperature gradient across the actuator beam (with dimension L), in a unit of watts (W) is obtained by: $K.(\partial^2 T/\partial \ell^2) + P_e = 0$. Where P_e is the electrical power converted to heat per volume (L). It is determined by: P_e $V{\cdot}I^2$ $L\cdot$ $\cdot$, where I is the current passing through the beam. Thermal conductivity is assumed as κ= 3.2×10^7 PW/(µm.K) for polysilicon, the actuator structural material. Solution of the above energy equation is a temperature distribution function given by $T(\ell) = c_1.\ell^2 + c_2.\ell + c$. Assuming equal heat flux at both ends, $(\partial T(0)/\partial \ell) + (\partial T(0)/\partial \ell) = 0$, and by applying desired boundary conditions, the coefficients of temperature distribution is determined as: c $T\ 0$ 300 K for ℓ 0, c_1 - P_e 2κ , and c_2 $-c_1 L_i$, For a chevron beam with a length $L_i \approx 2L_{hi}$ (ignoring joint width, w_g), the temperature change at joint of two symmetric hot arms is given by $\Delta T_i(\ell$ L_{hi} $-c_1.L_{hi}^2$ $P_e.L_{hi}^2$ 2κ , The heat distributions within the structure may vary by the configuration of the power applied to actuator anchors due to the electrical current path. Temperature distribution profile of the V-shape thermal actuator is demonstrated in Section 4.

2 3 Thermo-mechanical model and analysis

As discussed, the thermo-mechanical transduction is used as the actuation method for the V-shape actuator. The polysilicon structure has a coefficient of (linear) thermal expansion, α ΔL $L.\Delta T$, which quantifies the relative dimensional change of the actuator beams that occurs for a change in temperature, ΔT. Knowing that $\Delta T\ \ell$ $T\ \ell$ $-T\ 0$ $c_1.\ell^2$ $c_2.\ell$, for a chevron beam with a length $L_i \approx 2L_{hi}$ the length expansion ΔL_i is determined by

$$\Delta L_i(\ell) = \int_0^{\ell} \alpha.\Delta T_i(\ell).d\ell \tag{2}$$

The length expansion of the hot arm, ΔLh_i is half of ΔL_i L_i , and is calculated by: ΔL_{hi} $\alpha{\cdot}P_e$ $\cdot L_{hi}^3$ 3κ . The temperature coefficient α is 2.8×10^{-6} K^{-1}. The total displacement of the actuator tip is limited to the maximum displacement generated by the shortest chevron beam (arms $h2$-$h2$) and is determined by: Δ $_{total}$ Δ $_{h2}$ ΔL_{g12}. ΔL_{g12} is the length change of the joint g12 and ΔY_{h2} is the displacement of the joint beam generated by length expansion of the chevron beam of $h2$. Δ $_{h2}$ can be calculated by $\Delta\ _{h2} = (L_{h2}+\Delta L_{h2}).sin\left[cos^{-1}\left(L_{h2}.\cos(\theta)/(L_{h2}+\Delta L_{h2})\right)\right] - L_{h2}.\sin(\theta)$, where L_{h2}, ΔL_{h2} are the initial length, and the length change of the hot arm $h2$, respectively. Each chevron beam generates a force of $_i$ at the joint beam and can be determined by $_i = E.(w_{hi}/L_{hi})^3.\ .\Delta\ _{hi}/32$, where L_{hi}≈$0.5L_i$. The force $_i$ can be rewritten as $_i = E.\beta_{hi}^{-3}.w_{f1}^3.\ .L_{f1}^{-3}.\Delta\ _{hi}/32$ based on the design parameter discussed in this section. E is the polysilicon young's modulus, E 160 GPa. For hot arms with index number of i = 1 to n = 3, the total force of the three chevron beams, $_{total}$, generated by the displacement Δ $_{h2}$ is determined by

$$_{total} = \sum_{i=1}^{n=3}\ _{i+1} = \frac{1}{32}\left(\frac{w_{f1}}{L_{f1}}\right)^3 .E.\ \ \Delta\ _{h2}\cdot\left(\sum_{i=1}^{n=3}(\beta_{h2}+(i-1)\beta_d)^{-3}\right) \tag{3}$$

By adjusting the size ratio of the hot arm $h2$, the desired force of the actuator can be achieved. The heat distribution and actuator tip displacement profiles of the V-shape actuator are demonstrated in Section 4.

3 FABRICATION PROCESS

PolyMUMPS foundry service is employed for the device fabrication. The standard process flow is illustrated in Figure 4 [5]. A standard PolyMUMPS technology consists of five major layers; single crystal silicon (SCS) as device substrate, silicon nitride (SiN) as structural anchor and electrical isolation, polysilicon as structural material, silicon dioxide (SiO_2) as sacrificial layer, and Aluminum as routing and pad material.

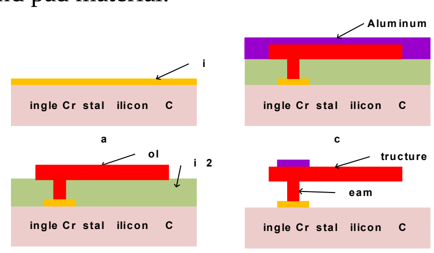

Figure 4: Actuator fabrication process

RESULTS

A general lumped-element model of the 4-arm V-shape actuator has been extracted and simulated using Matlab and CoventorWare FEA software. Figure 5 shows the simulated temperature distribution with a driving voltage of 1V. The maximum temperature is found to be ~500 K on the cold arm and the hot arm joints, which is considered a safe operation temperature for the actuator.

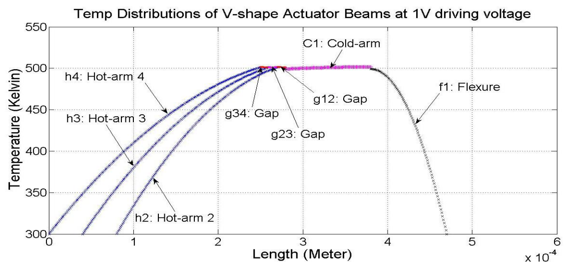

Figure 5: Temperature distribution in 4-arm V-shape actuators shown in Figure 1 at 1 V driving voltage.

The in-plane displacement of the actuator versus the increment of the supply voltage is illustrated in Figure 6. A close simulation results between both software indicates the accuracy of the actuator model derived in this work. At 1 V, ~2.7 µm of in-plane displacement is obtained.

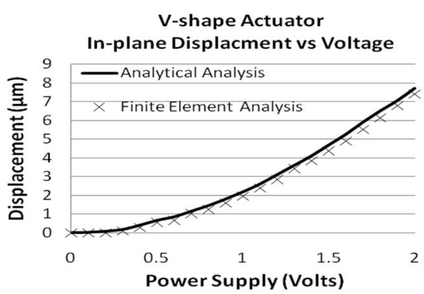

Figure 6: Displacement ~ voltage response of the 4-arm V-shape actuator of Figure 1 (a).

Figure 7 shows the out-of-plane (-axis) displacement of the actuator with 1 V voltage supply. Due to constrain of the four arms, a small -displacement of ~0.006 µm is observed, which satisfies our design requirement.

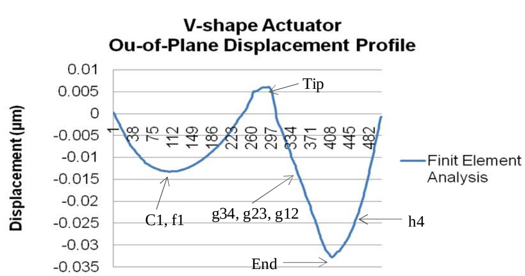

Figure 7: Out-of-plane displacement of the 4-arm V-shape actuator structure of Figure 1 (a).

Measurement on one actuator with configuration shown in Figure 1(b) was performed using a Veeco surface profilometer. At a 1.4 V driving voltage, simulation and FEA results show an in-plane displacement of 1.77 µm and 1.86 µm while Veeco measurement shows 1.4 µm. The result difference is due to neglecting the effects of heat loss from the convection and radiation in analysis and simulation.

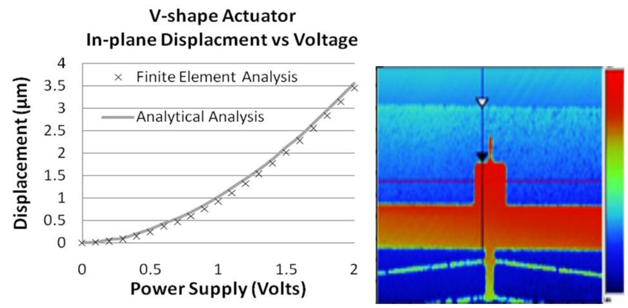

(a) (b)

Figure 8: (a) Simulated results, and (b) Veeco surface profilometer measurement.

5 DISCUSSIONS

A 4-arm V-shape actuator has been successfully modeled, simulated and fabricated. With a 1 V driving voltage, the actuators shown in Figure 1 (a) and (b) demonstrate respectively in-plane y-displacements of ~2.7 µm and ~1.0 µm, with force magnitudes ranging from 100 µN to 250 µN. The displacement results are almost one order times greater than the single-sided U-shape actuators reported in other literatures. Compared to single-sided U-shape actuators, these actuators also maintain a small out-of-plane displacement of less than ($\pm\Delta Z$) ~0.006 µm. Moreover, due to symmetrical structure, the V-shape actuators generate very small undesired in-plane lateral displacement ($\pm\Delta X$) of less than ~0.02 µm. At steady state, this actuator consumes a power of approximately 2.2 mW. The maximum temperature of 500 K is observed at joint and cooling arms. The FEA results are more than 95% in agreement with respective theoretical results.

REFERENCES

[1] C. Kung, R.S. Chen, *. of the Chinese Institute of Engineers*, Vol. 28, No. 1, (2005), pp. 123-130.
[2] Q. Huang, N. K. Shek Lee, *. of Micromech. Microeng.* 9, (1999), pp. 64-70.
[3] Y.S. Yang, Y.H. Lin, Y.C. Hu and C.H. Liu, *. of Micromech. and Microen.* 19 (2009) 015001, 12.
[4] J. Qiu, J. H. Lang, A.H. Slocum, A.C. Weber, *. f Microelectromech. Sys.* Vol. 14, (2005), 5.
[5] PolyMUMPs Design Handbook, Version 11.0, *www.memscap.com.*